Research Article

An Artificial Intelligence Regression Model for Prediction of NO_x Emission from Flame Image

Sedat Golgiyaz[1] iD *, Mahmut Daskin[2]* iD *, Cem Onat[3]* iD *, M. Fatih Talu[4]* iD

[1]*Department of Computer Engineering, Bingol University, Bingol, Turkey*
[2]*Department of Mechanical Engineering, Inonu University, Malatya, Turkey*
[3]*Department of Air-frame and Power Plant, Firat University, Elazig, Turkey*
[4]*Department of Computer Engineering, Inonu University, Malatya, Turkey*

ARTICLE INFO

ABSTRACT

In this study, NO_x emission has been estimated by processing the flame image of visible wavelength and its experimental verification has been presented. The experimental study has been performed by using a domestic coal boiler with a capacity of 85000 Kcal / h. The real NO_x value has been measured from a flue gas analyzer device. The flame image has been taken by CCD camera from the observation hole on the side of the burner. The data set which is related to instantaneous combustion performance and flame images was recorded simultaneously on the same computer with time stamps once a second. The color flame image has been transformed into a gray scale. Features have been extracted from the gray image of flame. The features are extracted by using the cumulative projection vectors of row and column matrices. ANN regression model has been used as the learning model. The relationship between flame image and NO_x emission has been obtained with the accuracy of R = 0.9522. Highly accurate measurement results show that the proposed NO_x prediction model can be used in combustion monitor and control systems.

1. Introduction

As a reliable and low-cost fossil fuel, coal is a strategic energy source in terms of energy security for the very country. Coal stands out as being the safest fossil fuel in terms of obtaining, storing, transporting and using. For this reason, coal is widely used both in domestic areas and industrial areas such as thermal power plants, glass, steel and cement industries. On the other hand, emission values of coal combustion systems are constantly being discussed due to environmental concerns. According to the World Energy Outlook 2017 [1] report published by IEA, it is stated that in 2016, 9.5 billion tons of CO2 (carbon dioxide) was emitted from coal-fired thermal power plants to the atmosphere. This rate corresponds to approximately 70% of the emission released from the conversion sector [2]. When we use coal in power plants, sulfur dioxide (SO2), particulate matter and nitrogen oxides (NOx) are released into the atmosphere. Therefore, measurement and control of the emission values stand out as an important and daily issue in order to increase efficiency in coal burning systems and to reduce their negative effects on the environment.

[1] Corresponding author
e-mail: sedatg@bingol.edu.tr

1.1. Motivation

In practice, emission values are traditionally made by flue gas analysis devices[3]. Recently, as an alternative method, measurement systems containing artificial intelligence based on flame image have been used [4]–[8]. Measurement mechanisms that make emission estimation by processing flame images are both cheaper systems and lower operating costs compared to their counterparts. In addition, dead time in control systems makes the controller design process extremely difficult [9]–[11]. Since the system created with flame images quickly reflect the combustion conditions, they constitute an important advantage that greatly minimizes the dead time in closed loop control systems [12], [13]. In particular, this feature provides a significant advantage from the control design perspective. These advantages offered by flame image-based measurement systems motivate engineers to design a more effective, flame image-based emission measurement system with higher accuracy.

1.2. Related Works

Emission estimation via CCD (Charge-Coupled Device) cameras is more advantageous systems compared to flue gas analyzer devices because they are inexpensive systems and do not require consumables. The use of computer vision systems in the industry is increasing day by day [14]–[18]. In general, there are three types of application performed by processing the flame image. The first is monitoring and controlling of the combustion process in burners [19]–[23], the second is estimation of the emission resulting from the combustion [24]–[27] and the last one is estimation of the temperature of the combustion chamber [28]–[30]. In addition to these types of applications, there are different studies. For example, coal type can be classified with the image of the flame [28]. In NOx emission prediction system performed with CCD cameras, available in some studies with color space of HSI (Hue, Saturation, Intensity) [25] as well as in color space of RGB (Red Green Blue) [24]. In a combustion process, there are many factors affecting NOx emissions. These factors have different effects on NOx emissions. To find the appropriate formula or mathematical model to predict the NOx emission from the coal boiler is very difficult. But, it is possible to estimate NOx emission using image

processing techniques and ANN regression model [24]. Because ANNs are very good at modeling the complex phenomena. It has been reported in [25] that there is a relationship between 30-65 bars and the emission level of NOx in the tone level histogram in the HSI color space. In studies which uses CCD cameras, radial energy emitted from the flame was used frequently to extract features from the image of flame [27], [31], [32]. In these studies, the Radial Energy Signal (RES) is calculated with the gray image of flame. A good study on combustor control with flame image is given in [31]. Here, NOx emission and thermal efficiency are optimized with the radiant energy signal obtained from the flame image [31]. [19] and [33] have made a nice contribution to those studying flame characterization by digital image processing on industrial scale burners. In the studies which are performed with colored flame images, the image is generally converted to gray level in order to reduce the dimension (to reduce the calculation load) and the feature is obtained from the gray level image [19], [20], [22], [31]. Similarly, there are studies with only one color (blue) channel [34] or only the tone component of the color image [25]. Flue gas analyzer is used in flue gas emission studies [35] and there are studies in which the concentration of radicals formed as a result of combustion is determined by spectroscopic imaging [26], [27], [36], [37][27], [36]. CCD cameras are preferred in emission estimation because they are both common and cheap [24], [25], [38]. When the studies mentioned above are subjected to a general evaluation, it is concluded that the subject of estimating the combustion emission values from the flame image is a current-trend field of study. The methods used in studies [22], [25], which came to the fore especially in NOx estimation, have been a significant result of the literature search.

1.3. Contribution

There are some challenging problems with studies of imaging the combustion chamber. Some of these are the large data size of the flame images and the problems of determining the meaningful features expressing the burning from these images. The operations to solve these problems increase the computational complexity. In addition, optimizing the appropriate modeling technique to reveal the relationship between the features obtained from the

flame image and the combustion process is another dimension of the problem. In this study, a new regression model is presented that reveals the relationship between flame image and NOx emission. The proposed model includes image processing techniques and artificial neural network elements. For emission estimation, the features are extracted out by using the flame image converted to gray level. Position dependent feature vectors are used to express the burning process better. For this purpose, cumulative projection vectors of row and column matrices are used to obtain the features. These simple and effective features are ideal for evaluating the flame in terms of brightness and volume. Using position dependent features also provides information about the homogeneity of the flame. The study performed in comparison with the NOx emission estimation methods [22], [25] that stand out in the literature, reveals the efficiency of the proposed estimation model.

1.4. Outline of the Paper

In the next Section, data collection process is explained. In Section 3, feature extraction from flame images is explained. In the Section 4, ANN model is designed. In Section 5, experimental results are presented in comparison with the methods mentioned in the literature. Eventually, the final section discusses experimental results. Also, clues about future studies have been given.

2. Data Collection

The experimental study has been carried out with a domestic burner system with a capacity of 85,000 kcal/h. Nut coal has been used as fuel in the experimental study. The schematic representation of the system is given in Figure 1. The system is constructed with a 10 cm diameter circular viewing window on the side of the burner. Combustion has been monitored by a CCD camera placed behind this window.
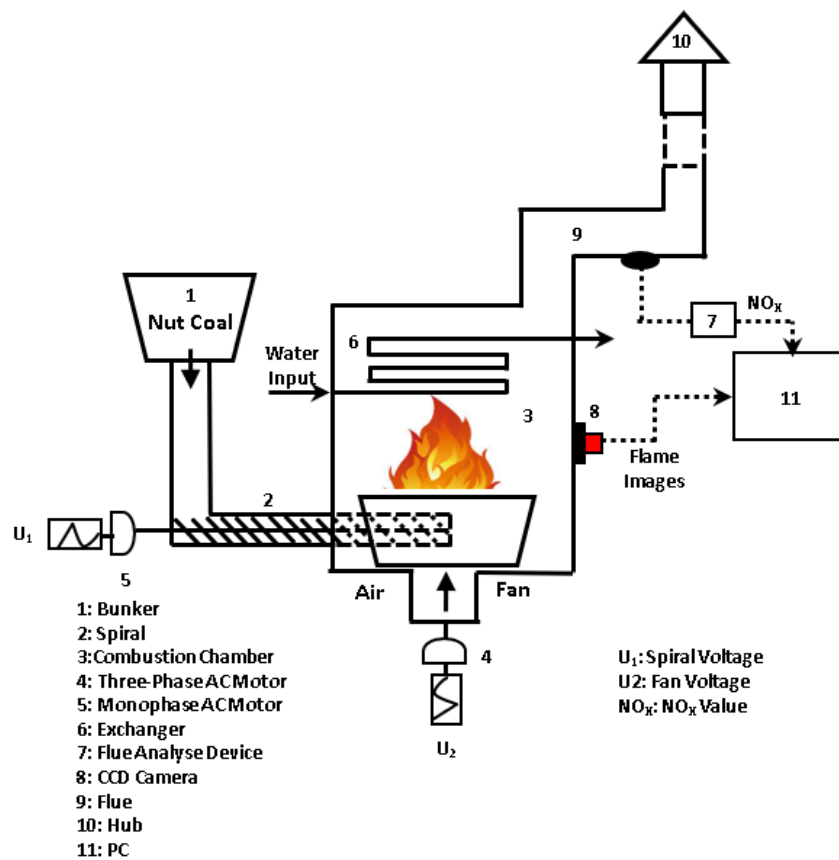

1: Bunker
2: Spiral
3: Combustion Chamber
4: Three-Phase AC Motor
5: Monophase AC Motor
6: Exchanger
7: Flue Analyse Device
8: CCD Camera
9: Flue
10: Hub
11: PC

U_1: Spiral Voltage
U_2: Fan Voltage
NO_x: NO_x Value

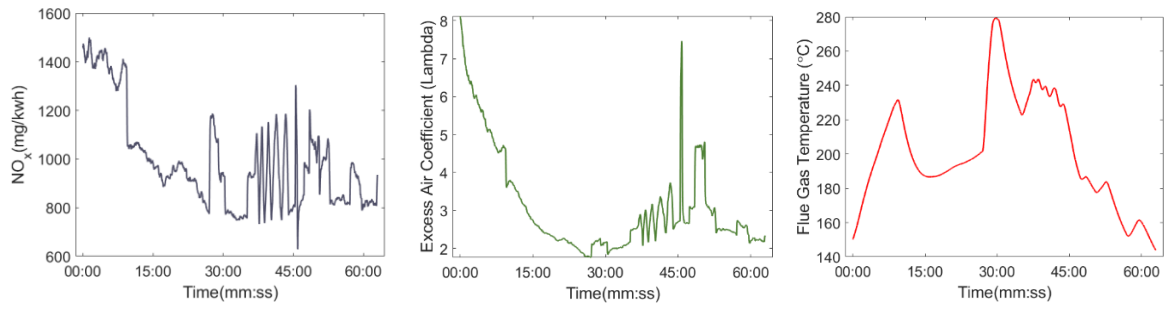**Figure 1** Schema of the burner system

Figure 2 Combustion conditions; (a) NO_x emissions; (b) excess air coefficient; (c) flue gas temperature

The combustion conditions at the time of obtaining experimental data are given in Figure 2. In order to illustrate all possible combustion conditions in the experimental composition, the combustion conditions have been adjusted to be in a wide range.

Different forms of expressions of a colored flame image obtained from the combustion chamber are given in Figure 3.
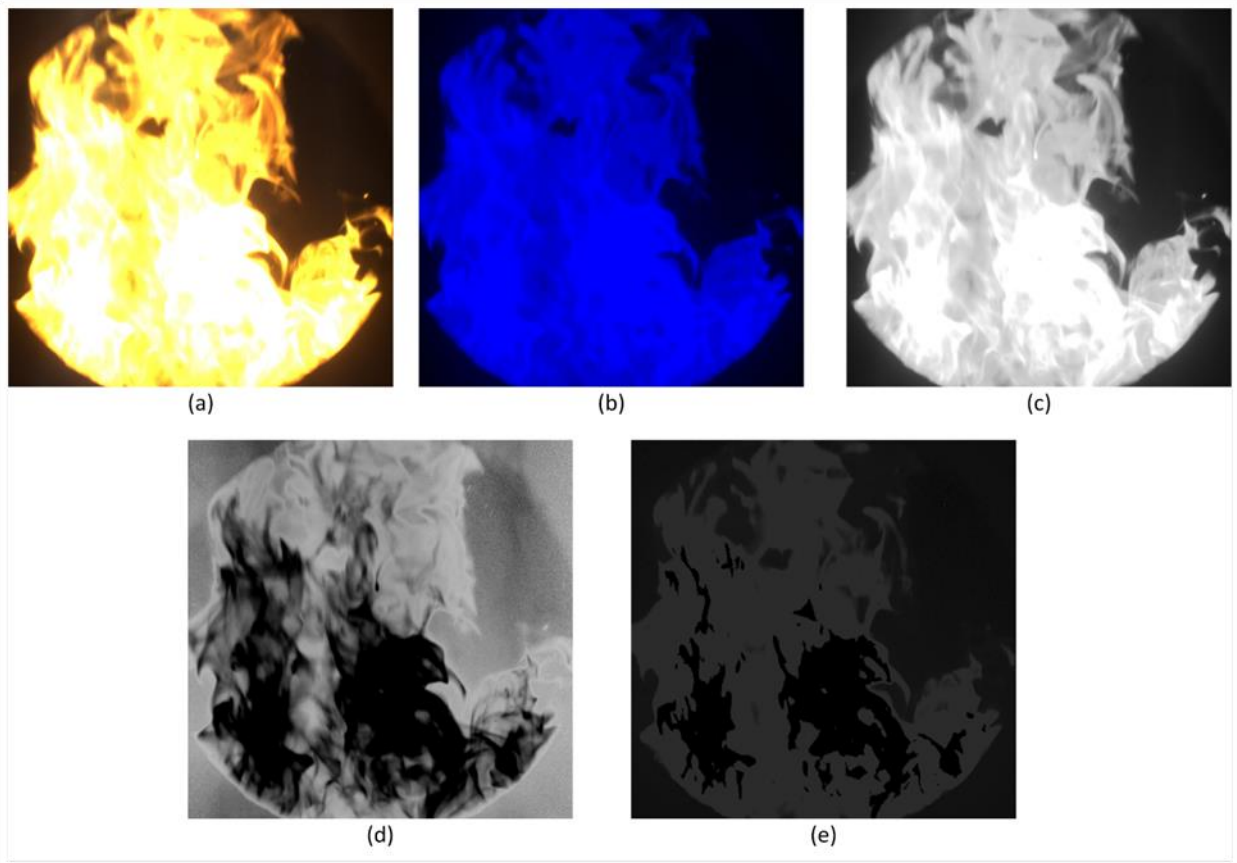

Figure 3 A flame image; (a) RGB and (b) HSI color spaces, (c) intensity (I), (d) saturation(S) and (e) hue (H) components

In this study, the gray level of the flame image in RGB color space has been used. The burning process has been monitored for 63 minutes by recording a single image per second at 1200 × 1200 resolution via a CCD camera. In addition, the NOx measurement value per second has been taken from the flue gas emission device synchronously with the flame images. The region of interest has been chosen so that the flame image is 1160 × 1160 pixels in size. The flame image obtained from the camera and the NOx value obtained from the flue gas analyzer have been recorded on the same computer with time labels. In this way, 3780 NOx measurement values and flame images have been collected simultaneously during the experiment.

In cases when it was not possible to obtain data from the camera or analyzer, the relevant data acquired at his time period have not been taken into consideration. The NOx

emission data obtained from the flue gas analyzer have been used as reference data in the training and testing stages of the model.

3. Feature Extraction

The main factors affecting NOx emissions in coal combustor systems are given below [39].
- Average temperature in the combustion chamber.
- Homogeneity of temperature in the combustion chamber.
- Gas residence time in high temperature zone.
- Air excess coefficient and property of coal.

There is a relationship between the flame image and the factors affecting NOx emissions [17], [24], [27]. Therefore, the relationship between flame image and NOx emission can be revealed by image processing and machine learning techniques. In this study, cumulative horizontal and vertical projection vectors are used to extract attributes from the flame image.

3.1. Horizontal-Vertical Projection Vectors

Cumulative horizontal and vertical projection vectors can be calculated as in Equation 1-2. Here $I_{m \times n}$ is the gray level image of the flame.

$$X_{csum}^k = \sum_{j=1}^{k} \sum_{i=1}^{n} I_{ij} , 1 \leq k \leq m \qquad (1)$$

$$Y_{csum}^t = \sum_{i=1}^{t} \sum_{j=1}^{m} I_{ij} , 1 \leq t \leq n \qquad (2)$$

X_{csum}^k and Y_{csum}^t have been used together for training of the proposed system. Features and density information of the flame image were obtained depending on the location. Not only does density information represent the flame characteristic, but also includes positional information, expressing the combustion process better.

3.2. Relationship Between Hue Level and Combustion

Color HSI image consists of three components such as brightness, hue, and saturation. The conversion process from RGB color space to HSI color space is expressed using Equation 3-4.

$$r = \frac{R}{R+G+B}, \ g = \frac{G}{R+G+B}, \ b = \frac{B}{R+G+B} \qquad (3)$$

$$h = cos^{-1}\left(\frac{0.5*((r-g)+(r-b))}{((r-g)^2+(r-b)+(g-b))^{1/2}}\right) \qquad (4)$$

Here, if $b \leq g \ then$ h $\in [0,\pi]$

$$h = 2\pi - cos^{-1}\left(\frac{0.5*((r-g)+(r-b))}{\sqrt{(r-g)^2+(r-b)+(g-b)}}\right) \qquad (5)$$

Here, if $b > g \ then$ h $\in [\pi, 2\pi]$,

$$s = 1 - 3 * min(r,g,b) ; \ s \in [0,1] \qquad (6)$$

$$I = \frac{R+G+B}{3*255} ; \ I \in [0,1]. \qquad (7)$$

In [25], it has been reported that with the tone level of the flame, the light field can represent the dominant wavelength. Also, with regard to a luminous substance, it has been stated that there is a relationship between wavelength and tone level [40]. This relationship can be expressed as in Equation 8.

$$W = \frac{W_{max}-W_{min}}{2^d} Hue + W_{max} \qquad (8)$$

In this equation, W is the wavelength and d is the bit depth of the image. Wmax and Wmin values are 700nm and 400nm respectively. For normal images d = 8. Light undergoes radical luminescence with substances such as OH, CH, CO_2, NO_2, CO and H_2O.

4. Artificial Neural Networks

ANNs are mathematical machine learning models inspired by the biological behavior of nerve cells in the human body and the structure of the brain. In this study, a multi-layer perceptron (MLP) approach consisting of at least three layers called input, latent and output layer is used to estimate NOx emission. During the training phase, the features gathered from the flame images constitute the input and the NOx emission measured with the analyzer is used as the desired output. Coefficients of ANN are optimized according to the inputs and the output. A part of the data set is used for verification during the training phase. In the last stage, the rest of the data set is used to test the performance of the model. The rate of the data set used for training, testing and verification is given in Table 1. In the ANN regression model, the number of neurons in the hidden layer was taken as 8.
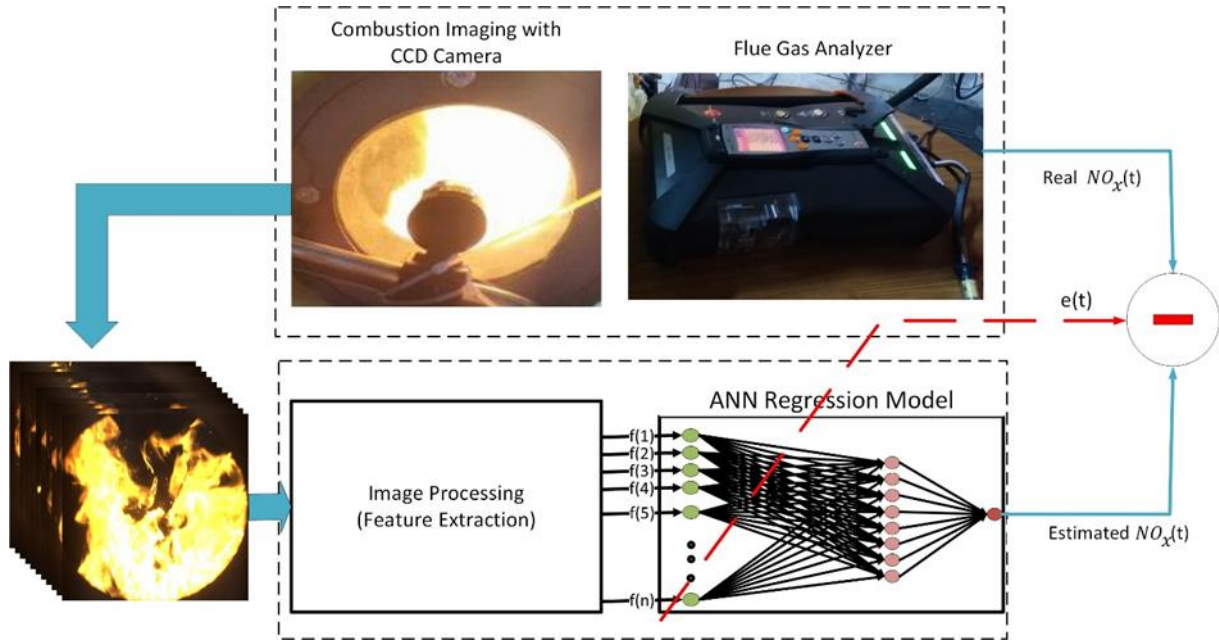
Figure 4. Block diagram of the proposed measurement system

Table 1. Separation of data in percentages for training, testing and validation

	All	**Training**	**Validation**	**Test**
Data Rate	%100	%70	%15	%15
Data number	3780	2646	567	567

In general, the initial weights are randomly selected in ANN and the weights are optimized by minimizing the cost function given in equation 9.

$$J(\theta) = \frac{1}{2N}\sum_{i=1}^{N}\left(h_\theta\left(x^{(i)}\right) - y^{(i)}\right)^2 \qquad (9)$$

Many training algorithms for ANN have been reported in the practice. The appropriate training algorithm varies according to many factors. Factors such as the complexity of the problem, the number of data points in the training set, the weight in the network and the number of biases determine the selection of the training algorithm. In the next section, the effects of different learning algorithms on the accuracy of the regression model have been also speculated.

4.1. Performance Metrics for Regression Model

Root mean square error (RMSE) and correlation coefficient (R) criteria were used to reveal the regression performance obtained during the training, validation and testing phases. R and RMSE values are defined by expressions given in Equations 10 and 11, respectively.

$$RMSE = \left[\frac{1}{N}\sum_{i=1}^{N}\left(D_i - \widetilde{D}_i\right)^2\right]^{1/2} \qquad (10)$$

$$R = \left[1 - \frac{\sum_{i=1}^{N}(D_i - \widetilde{D}_i)^2}{\sum_{i=1}^{N}(D_i - \overline{D})^2}\right]^{1/2} \qquad (11)$$

Here, D_i and $\overline{D}$ values represent the individual NOx emission value and the average of all D_i values, respectively. In addition, $\widetilde{D}_i$ represents the NOx emission value calculated as a result of ANN regression model.

5. Experimental Results

With the designed system, the NOx value measured by the flue gas analyzer has been regressed with the ANN model using the flame image. The NOx value obtained from the flue gas analyzer has been taken as a reference value in the proposed system and used in the training and testing phase.

The results obtained for comparison have been run ten times for all models. The results presented in Table 2 are the average values of these 10 runs. In order to demonstrate the performance of the proposed feature extraction method better, the results of other feature extraction methods presented for NOx emission in the literature with the same data set and the same ANN architecture are comparatively given in Table 2. Training all the proposed methods for the same model and parameters in the same data set provided objective results in terms of comparing the

effectiveness of the methods. Accordingly, the proposed ANN regression model estimated the NOx emission with at least R = 0.9522 accuracy. The results obtained as a result of the experimental study revealed the effectiveness of the proposed feature extraction method.

While comparing the results, the results of four ANN learning models (LM, BFG, CGF and SCG) are given for proposed feature extraction method and other methods. Considering the results obtained, LM (Levenberg-Marquardt) method gave better results despite the high memory requirement. BFG (BFGS Quasi-Newton), CGF (Fletcher-Powell, Conjugate

Gradient) and SCG (Scaled Conjugate Gradient) methods have been performed faster than LM. However, accuracy is not at the desired level in these methods. Although [25] reported a direct relationship between NOx emission and the tone histogram [30-65] bars, the relation in this study became clear between the bar bars of the histogram [0-85]. 16 cameras have been used in [22] given in Table 2. The feature extraction method presented in [22] is presented for a single camera with the data in this study.

Table 2 Proposed method and other methods' result for same data set and ANN architecture

	Features	Training Algorithm	RMSE	R
Proposed	X_{csum}, Y_{csum}	LM	**59,566**	**0,952**
	X_{csum}, Y_{csum}	BFG	99,896	0,863
	X_{csum}, Y_{csum}	CGF	94,072	0,879
	X_{csum}, Y_{csum}	SCG	95,941	0,874
Others	Histogram (0-85) [25]	LM	91,581	0,886
	Histogram (30-65)[25]	LM	121,544	0,789
	Histogram (0-85) [25]	BFG	121,916	0,787
	Histogram (30-65) [25]	BFG	143,506	0,687
	Histogram (0-85) [25]	CGF	120,741	0,789
	Histogram (30-65) [25]	CGF	145,904	0,672
	Histogram (0-85) [25]	SCG	116,810	0,805
	Histogram (30-65) [25]	SCG	142,704	0,691
	μ [22]	LM	176,640	0,451
	μ [22]	BFG	177,876	0,438
	μ [22]	CGF	178,668	0,430
	μ [22]	SCG	178,187	0,435

In Figure 5, the NOx values produced by using of flame images with the proposed measurement system and the NOx values obtained from the flue gas analyzer are given. It is seen from this picture that the proposed measurement system is capable of estimating NOx emissions with at least 95% accuracy in all combustion conditions.
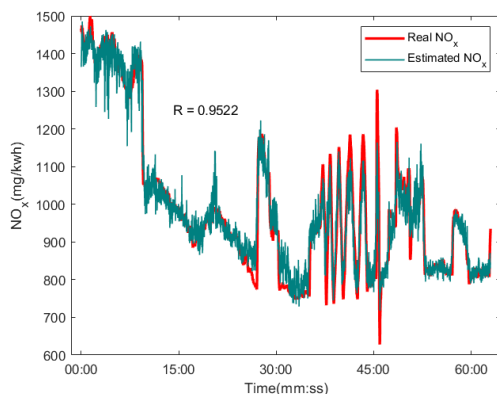

Figure 5 Performance of the proposed model

6. Conclusion

In this study, a new measurement system is proposed for the problem of estimating NOx emission from the flame image in the coal combustion process. When the obtained results are evaluated, the NOx estimation system established with the proposed method gives more successful results than other methods reported in the literature. Since CCD cameras are both cheap and common, the measurement structure presented in this study is advantageous in terms of cost. It also provides an option that minimizes the time delay in establishing closed loop combustion control systems. Within the scope of this domestic scale study, the proposed system can be extended for emission estimation in the industry. For future emission estimation studies, both the feature extraction phase and the learning models' phase are open to development.

References

[1] The U.S. Energy Information Administration (EIA), "International Energy Outlook 2017." Accessed: Oct. 22, 2018. [Online]. Available: www.eia.gov/ieo.

[2] J. Diefenderfer, M. assumptions Vipin Arora, and L. E. Singer, *International Energy Outlook 2016*, vol. 0484, no. May. 2016.

[3] X. Qiu, L. Duan, Y. Duan, B. Li, D. Lu, and C. Zhao, "Ash deposition during pressurized oxy-fuel combustion of Zhundong coal in a lab-scale fluidized bed," *Fuel Process. Technol.*, vol. 204, p. 106411, Jul. 2020, doi: 10.1016/j.fuproc.2020.106411.

[4] R. Weber and M. Mancini, "On scaling and mathematical modelling of large scale industrial flames," *J. Energy Inst.*, vol. 93, no. 1, pp. 43–51, Feb. 2020, doi: 10.1016/j.joei.2019.04.010.

[5] W. Wójcik, B. Suleimenov, M. J.-J. of Ecological …, and undefined 2017, "Employing Optical Measurements for Monitoring and Diagnostics of Combustion Process in Industrial Conditions," *yadda.icm.edu.pl*, vol. 18, no. 1, pp. 273–283, 2017, doi: 10.12911/22998993/67107.

[6] C. Onat and M. Daskin, "A basic ANN system for prediction of excess air coefficient on coal burners equipped with a CCD camera," *Math. Stat.*, vol. 7, no. 1, pp. 1–9, 2019, doi: 10.13189/ms.2019.070101.

[7] C. Onat, M. Daşkin, S. Toraman, S. Golgiyaz, and M. F. Talu, "Prediction of combustion states from flame image in a domestic coal burner," *Meas. Sci. Technol.*, vol. 32, no. 7, p. 075403, Jul. 2021, doi: 10.1088/1361-6501/abe446.

[8] S. Golgiyaz, M. F. Talu, and C. Onat, "Estimation of Excess Air Coefficient for Automated Feed Coal Burners with Image-Based Gauss Model," in *International Artificial Intelligence and Data Processing Symposium (IDAP'16)*, 2016, pp. 528–531, [Online]. Available: https://www.researchgate.net/publication/333650492.

[9] C. Onat, "A new concept on PI design for time delay systems: weighted geometrical center," *J. Innov. Comput. Inf. Control*, 2013.

[10] C. Onat, "WGC Based Robust and Gain Scheduling PI Controller Design for Condensing Boilers," 2014, doi: 10.1155/2014/659051.

[11] C. Onat, "A new design method for PI–PD control of unstable processes with dead time," *ISA Trans.*, vol. 84, pp. 69–81, 2019, doi: 10.1016/j.isatra.2018.08.029.

[12] C. Katzer, K. Babul, M. Klatt, and H. J. Krautz, "Quantitative and qualitative relationship between swirl burner operatingconditions and pulverized coal flame length," *Fuel Process. Technol.*, vol. 156, pp. 138–155, 2017, doi: 10.1016/j.fuproc.2016.10.013.

[13] S. Taamallah, N. W. Chakroun, H. Watanabe, S. J. Shanbhogue, and A. F. Ghoniem, "On the characteristic flow and flame times for scaling oxy and air flame stabilization modes in premixed swirl combustion," *Proc. Combust. Inst.*, vol. 36, no. 3, pp. 3799–3807, 2017, doi: 10.1016/j.proci.2016.07.022.

[14] J. Li, M. M. Hossain, J. Sun, Y. Liu, … B. Z.-A. T., and undefined 2019, "Simultaneous measurement of flame temperature and absorption coefficient through LMBC-NNLS and plenoptic imaging techniques," *Elsevier*.

[15] T. Lockwood, "Advanced sensors and smart controls for coal-fired power plant controls for coal-fired power plant," no. June, 2015, [Online]. Available: https://www.usea.org/sites/default/files/media/Advance sensors and smart controal for coal fired power plants - ccc251.pdf.

[16] J. Ballester and T. García-Armingol, "Diagnostic techniques for the monitoring and control of practical flames," *Prog. Energy Combust. Sci.*, vol. 36, no. 4, pp. 375–411, 2010, doi: 10.1016/j.pecs.2009.11.005.

[17] S. Golgiyaz, M. F. Talu, and C. Onat, "Artificial neural network regression model to predict flue gas temperature and emissions with the spectral norm of flame image," *Fuel*, vol. 255, p. 115827, Nov. 2019, doi: 10.1016/j.fuel.2019.115827.

[18] S. Golgiyaz, M. F. Talu, and C. Onat, "Estimation of Flue Gas Temperature by Image Processing and Machine Learning Methods," *Eur. J. Sci. Technol.*, pp. 283–291, Aug. 2019, doi: 10.31590/ejosat.568348.

[19] A. González-Cencerrado, B. Peña, and A. Gil, "Coal flame characterization by means of digital image processing in a semi-industrial scale PF swirl burner," *Appl. Energy*, vol. 94, pp. 375–384, 2012, doi: 10.1016/j.apenergy.2012.01.059.

[20] A. González-Cencerrado, A. Gil, and B. Peña, "Characterization of PF flames under different swirl conditions based on visualization systems," *Fuel*, vol. 113, pp. 798–809, Nov. 2013, doi: 10.1016/j.fuel.2013.05.077.

[21] Z. Xiangyu, Z. Shu, Z. Huaichun, Z. Bo, W. Huajian, and X. Hongjie, "Simultaneously reconstruction of inhomogeneous temperature and radiative properties by radiation image processing," *Int. J. Therm. Sci.*, vol. 107, pp. 121–130, 2016, doi: 10.1016/j.ijthermalsci.2016.04.003.

[22] Z. Liu, S. Zheng, Z. Luo, and H. Zhou, "A new method for constructing radiative energy signal in a coal-fired boiler," *Appl. Therm. Eng.*, vol. 101, pp. 446–454, 2016, doi: 10.1016/j.applthermaleng.2016.01.034.

[23] P. Tóth, A. Garami, and B. Csordás, "Image-based deep neural network prediction of the heat output of a step-grate biomass boiler," *Appl. Energy*, vol. 200, pp. 155–169, Aug. 2017, doi: 10.1016/j.apenergy.2017.05.080.

[24] F. Wang *et al.*, "The research on the estimation for the NOxemissive concentration of the pulverized coal boiler by the flame image processing technique," *Fuel*, vol. 81, no. 16, pp. 2113–2120, 2002, doi: 10.1016/S0016-2361(02)00145-X.

[25] W. B. Baek, S. J. Lee, S. Y. Baeg, and C. H. Cho, "Flame image processing & analysis for optimal coal firing of thermal power plant," *{ISIE 2001 IEEE Int. Symp. Ind. Electron. proceedeing, Vols I-III}*, p. {928-931}, 2001, doi: 10.1109/ISIE.2001.931596.

[26] X. Li, D. Sun, G. Lu, J. Krabicka, and Y. Yan, "Prediction of NOx emissions throughflame radical imaging and neural network based soft computing," *IST 2012 - 2012 IEEE Int. Conf. Imaging Syst. Tech. Proc.*, vol. 44, no. 0, pp. 502–505, 2012, doi: 10.1109/IST.2012.6295594.

[27] N. Li, G. Lu, X. Li, and Y. Yan, "Prediction of NOx Emissions from a Biomass Fired Combustion Process Based on Flame Radical Imaging and Deep Learning Techniques," *Combust. Sci. Technol.*, vol. 188, no. 2, pp. 233–246, 2016, doi: 10.1080/00102202.2015.1102905.

[28] Q. Tang, H. Zhou, G. Lu, Y. Yan, and Y. Li, "Combining flame monitoring techniques and support vector machine for the online identification of coal blends," *J. Zhejiang Univ. A*, pp. 671–689, 2017, doi: 10.1631/jzus.a1600454.

[29] Z. Xiangyu, L. Xu, Y. yu, Z. Bo, and X. Hongjie, "Temperature measurement of coal fired flame in the cement kiln by raw image processing," *Meas. J. Int. Meas. Confed.*, 2018, doi: 10.1016/j.measurement.2018.07.063.

[30] T. Li, C. Zhang, Y. Yuan, Y. Shuai, and H. Tan, "Flame temperature estimation from light field image processing," *Appl. Opt.*, vol. 57, no. 25, p. 7259, 2018, doi: 10.1364/ao.57.007259.

[31] B. Huang, Z. Luo, and H. Zhou, "Optimization of combustion based on introducing radiant energy signal in pulverized coal-fired boiler," *Fuel Process. Technol.*, vol. 91, no. 6, pp. 660–668, Jun. 2010, doi: 10.1016/j.fuproc.2010.01.015.

[32] Z. Huaichun and C. han, "An Exploratory Investigation of the Computer-Based Control of Utility Coal-Fired Boiler Furnace Combustion," *J. Eng. Therman Enegry Power*, 1994.

[33] D. Castiñeira, B. C. Rawlings, and T. F. Edgar, "Multivariate image analysis (MIA) for industrial flare combustion control," *Ind. Eng. Chem. Res.*, vol. 51, no. 39, pp. 12642–12652, 2012, doi: 10.1021/ie3003039.

[34] M. F. Talu, C. Onat, and M. Daskın, "Prediction of Excess Air Factor in Automatic Feed Coal Burners by Processing of Flame Images," *Chinese J. Mech. Eng.*, vol. 30, no. 3, pp. 722–731, May 2017, doi: 10.1007/s10033-017-0095-3.

[35] C. Moon, Y. Sung, S. Eom, and G. Choi, "NOx emissions and burnout characteristics of bituminous coal, lignite, and their blends in a pulverized coal-fired furnace," *Exp. Therm. Fluid Sci.*, vol. 62, no. 1, pp. 99–108, 2015, doi: 10.1016/j.expthermflusci.2014.12.005.

[36] J. Krabicka, G. Lu, and Y. Yan, "A spectroscopic imaging system for flame radical profiling," in *2010 IEEE Instrumentation & Measurement Technology Conference Proceedings*, 2010, pp. 1387–1391, doi: 10.1109/IMTC.2010.5488056.

[37] N. Li, G. Lu, X. Li, Y. Y.-I. T. on Instrumentation, and undefined 2015, "Prediction of pollutant emissions of biomass flames through digital imaging, contourlet transform, and support vector regression modeling," *ieeexplore.ieee.org*.

[38] S. Zheng, Z. Luo, Y. Deng, and H. Zhou, "Development of a distributed-parameter model for the evaporation system in a supercritical W-shaped boiler," *Appl. Therm. Eng.*, vol. 62, no. 1, pp. 123–132, 2014, doi: 10.1016/j.applthermaleng.2013.09.029.

[39] H. C. Zeng, *Combustion and pollution*. Wuhan: Publishing Company of Huazhong University of Science and Technology, 1992.

[40] J. A. Dean, *Flame photometry*. McGraw-Hill series in advanced chemistry., 1960.